THE ASTROPHYSICAL JOURNAL, 521:630–639, 1999 August 20

SCALE-FREE EQUILIBRIA OF ISOPEDIC POLYTROPIC CLOUDS

D. GALLI,[1] S. LIZANO,[2] Z. Y. LI,[3] F. C. ADAMS,[4] AND F. H. SHU[5]

Received 1998 December 4; accepted 1999 March 31

ABSTRACT

We investigate the equilibrium properties of self-gravitating magnetized clouds with polytropic equations of state with negative index n. In particular, we consider scale-free isopedic configurations that have constant dimensionless spherical mass-to-flux ratio λ_r and that may constitute "pivotal" states for subsequent dynamical collapse to form groups or clusters of stars. For given $\Gamma = 1 + 1/n$, equilibria with smaller values of λ_r are more flattened, ranging from spherical configurations with $\lambda_r = \infty$ to completely flattened states for $\lambda_r = 1$. For a given amount of support provided by the magnetic field as measured by the dimensionless parameter H_0, equilibria with smaller values of Γ are more flattened. However, logatropic (defined by $\Gamma = 0$) disks do not exist. The only possible scale-free isopedic equilibria with logatropic equation of state are spherical uniformly magnetized clouds.

Subject headings: ISM: clouds — ISM: magnetic fields — MHD — stars: formation

1. INTRODUCTION

The stage leading up to dynamic collapse of a magnetically subcritical cloud core to a protostar or a group of protostars is believed to be largely quasi-static if the responsible process is ambipolar diffusion (e.g., Mestel & Spitzer 1956; Nakano 1979; Lizano & Shu 1989; Tomisaka et al. 1989; Basu & Mouschovias 1994).[6] To describe the transition between quasi-static evolution by ambipolar diffusion and dynamical evolution by gravitational collapse, Li & Shu (1996) introduced the idea of a pivotal state, with the scale-free, magnetostatic, density distribution approaching $\rho \propto r^{-2}$ for an isothermal equation of state (EOS) when the mass-to-flux ratio has a spatially constant value, a condition that Shu & Li (1997) and Li & Shu (1997) termed "isopedic." Numerical simulations of the contraction of magnetized clouds justify the assumption of a nearly constant mass-to-flux ratio in the pivotal core.[7]

The small dense cores of molecular clouds that give rise to low-mass star formation are effectively isothermal (Myers & Benson 1983; Shu, Adams, & Lizano 1987). The situation may be different for larger regions that yield high-mass or clustered star formation. It has often been suggested that the EOS relating the gas pressure P to the mass density ρ of interstellar clouds can be represented by a polytropic relation $P \propto \rho^{1+1/n}$ with negative index n. Shu et al. (1972) pointed out the utility of this idealization within the context of the classic two-phase model of the diffuse interstellar medium (Pikel'ner 1967; Field, Goldsmith, & Habing 1969; Spitzer & Scott 1969), while Viala & Horedt (1974) published extensive tables analyzing the stability of nonmagnetized, self-gravitating spheres of such gases. Maloney (1988) examined the relation of line width size to density size in molecular clouds, first found by Larson (1981) and subsequently studied by many authors (e.g., Leung, Kutner, & Mead 1982; Torrelles et al. 1983; Dame et al. 1986; Falgarone et al. 1992; Miesch & Bally 1994). Maloney pronounced the results consistent with the properties of negative index polytropes. For a polytropic EOS, the sound speed $c_s \equiv (dP/d\rho)^{1/2} \propto \rho^{1/2n}$ increases with decreasing density if $n < 0$. The latter behavior may be compared with the empirical line width–density relation for molecular clouds, $\Delta v \propto \rho^{-q}$, with $q \simeq 0.5$ for low-mass cores (Myers & Fuller 1992) and $q \simeq 0.15$ for high-mass cores (Caselli & Myers 1995), which implies that n lies between -1 and -3, or that a static $\Gamma \equiv 1 + 1/n$ lies between 0 and 0.7.

The case $\Gamma = 1/2$ is of particular relevance for the equilibrium properties of molecular clouds. Walén (1944) found that the pressure of Alfvén waves propagating in a stratified medium, $P_{\rm wave} \propto |\delta \boldsymbol{B}|^2$, in the absence of damping obeys the simple polytropic relation $P_{\rm wave} \propto \rho^{1/2}$, a consequence of conservation of the wave energy flux $v_A |\delta \boldsymbol{B}|^2$. This result was later derived more rigorously by Weinberg (1962) in the WKB approximation for MHD waves propagating in mildly inhomogeneous media and, more recently, by Fatuzzo & Adams (1993) and McKee & Zweibel (1995) in a specific astrophysical context. In numerical simulations of the same problem, Gammie & Ostriker (1996) found indication of a much shallower relation ($\Gamma \simeq 0.1$) for a self-gravitating medium supported by nonlinear Alfvén waves. On the other hand, for the adiabatic contraction of a cloud supported by linear Alfvén waves, McKee & Zweibel (1995) found a dynamic γ larger than 1. Vázquez et al. (1998) confirmed a similar behavior in numerical simulations of the gravitational collapse of clouds with an initial field of hydrodynamic rather than hydromagnetic turbulence.

[1] Osservatorio di Arcetri, Largo E. Fermi 5, 50125, Firenze, Italy.

[2] Instituto de Astronomía, UNAM, Apdo. 70264, 04510 México D. F., México.

[3] Astronomy Department, University of Virginia, Charlottesville, VA 22903.

[4] Physics Department, University of Michigan, Ann Arbor, MI 48109.

[5] Astronomy Department, University of California, Berkeley, CA 94720-3411.

[6] For example, as measured either by the net accelerations or by the square of the inward flow speed divided by the sound speed, the ambipolar diffusion models in Figs. 3 and 6 of Ciolek & Mouschovias (1994) spend less than 0.1% of the total computed evolutionary time in states where even a single grid point is more than 10% out of mechanical balance with self-gravity, magnetic forces, and thermal pressure (see also Figs. 3 and 7 of Basu & Mouschovias 1994 and Fig. 1 of Ciolek & Königl 1998).

[7] For example, inside the starred point where Ciolek & Mouschovias (1994) consider the core to begin, the mass-to-flux ratio varies in the last models of their Figs. 3 and 6 by a factor of only 3 or 2 over a range in which the density varies by a factor $\sim 10^5$. Outside the starred point, the mass-to-flux value exhibits greater variation, but this occurs only because Ciolek & Mouschovias (1994) impose starting values for the mass-to-flux in the envelope that are $\sim 2 \times 10^{-2}$ times the critical value (see also Figs. 4a and 8b in Basu & Mouschovias 1994). Such small ratios for the bulk of the mass of a molecular cloud are probably ruled out by the Zeeman OH measurements summarized by Crutcher (1998).

In the limit of $\Gamma \to 0$ (or $n \to -1$), the EOS becomes "logatropic," $P \propto \ln \rho$, a form first used by Lizano & Shu (1989) to mimic the nonthermal support in molecular clouds associated with the observed supersonic line widths. The sound speed associated with the nonthermal contribution, $c_s = (dP/d\rho)^{1/2} \propto \rho^{-1/2}$, becomes important at the low densities characteristic of molecular cloud envelopes (as contrasted with the cloud cores) since the thermal contribution is independent of density if the temperature T remains constant. This nonthermal contribution decreases with increasing density and will become subsonic at high densities, as recently observed in the central regions of dense cores (Barranco & Goodman 1998). McLaughlin & Pudritz (1996) and McLaughlin & Pudritz (1997) have modeled the equilibrium and collapse properties of unmagnetized, self-gravitating spheres with a pure logatropic EOS and claim to find good agreement with observations.

Adams, Lizano, & Shu (in 1987) independently obtained the similarity solution for the gravitational collapse of an unmagnetized singular logatropic sphere (SLS), but they chose not to publish their findings until they had learned how to magnetize the configuration in a nontrivial way (see the reference to this work in Fuller & Myers (1992), who considered the practical modifications to the protostellar mass-infall rate introduced by "nonthermal" contributions to the support against self-gravity). Magnetization constitutes an important program to carry out if we try to justify a nonthermal EOS as the result of a superposition of propagating MHD waves (see also Holliman & McKee 1993). In this paper, we extend the study of Li & Shu (1996) to include the isopedic magnetization of pivotally self-gravitating clouds with a polytropic equation of state. As a by-product of this investigation, we obtain the unanticipated and ironic result that the only way to magnetize a singular logatropic configuration and maintain a scale-free equilibrium is to do it trivially, i.e., by threading the SLS with straight and uniform field lines (see § 6).

A basic consequence of treating the turbulence as a scalar pressure, coequal to the thermal pressure except for satisfying a different EOS, is that we do not change the basic topology of the magnetic field. This assumption may require reassessment if MHD turbulence enables fast magnetic reconnection (Vishniac & Lazarian 1999) and allows the magnetic fields of highly flattened cloud cores (Mestel & Strittmatter 1967; Barker & Mestel 1996) or pseudodisks (Galli & Shu 1993b) to disconnect from their background. Recent MHD simulations carried out in multiple spatial dimensions (e.g., Stone, Ostriker, & Gammie 1998; Mac Low et al. 1998; Ostriker, Gammie, & Stone 1999; Padoan & Nordlund 1999) find turbulence in strongly magnetized media to decay almost as fast as in unmagnetized media. Such decay may be responsible for accelerating molecular cloud core formation above simple ambipolar diffusion rates (Nakano 1998; Myers & Lazarian 1998; Shu et al. 1999). Although this result also cautions against treating turbulence on an equal footing as thermal pressure, we attempt a simplified first analysis that includes magnetization to assess the resulting configurational changes when we adopt an alternative EOS for the pivotal state. In particular, different power-law dependences of the radial density profile translate immediately to different time dependences in the mass-infall rate for the subsequent inside-out collapse (Cheng 1978; McLaughlin & Pudritz 1997).

The paper is organized as follows. In § 2 we formulate the equations of the scale-free problem and show that each solution depends only on the polytropic exponent Γ and a nondimensional parameter H_0 related to the cloud's morphology. In § 3 we present the numerical results. In § 4, § 5, and § 6 we discuss the limiting form of the solutions. Finally, in § 7 we give our conclusions and discuss the possible implications of our results for star formation and the structure of giant molecular clouds.

2. SELF-SIMILAR MAGNETOSTATIC EQUILIBRIUM EQUATIONS

To begin, we generalize the singular polytropic sphere in the same way that Li & Shu (1996) generalized the singular isothermal sphere (SIS). In the absence of an external boundary pressure, the only place the pressure P enters in the equations of magnetostatic equilibrium is through a gradient. Consider then the polytropic relation

$$\frac{dP}{d\rho} = K\rho^{-(1-\Gamma)} . \tag{1}$$

By integrating equation (1) we recover the isothermal EOS, $P = K\rho$ for $\Gamma = 1$ (where K is the square of the isothermal sound speed), and the logatropic EOS, $P = K \ln \rho$, for $\Gamma = 0$.

We adopt axisymmetry in spherical coordinates and consider a poloidal magnetic field given by

$$\boldsymbol{B} = \frac{1}{2\pi} \nabla \times \left(\frac{\Phi}{r \sin \theta} \hat{e}_\phi \right), \tag{2}$$

where $\Phi(r, \theta)$ is the magnetic flux. Force balance along field lines requires

$$V + \frac{1}{\Gamma - 1} K\rho^{-(1-\Gamma)} = h(\Phi) , \tag{3}$$

where V is the gravitational potential and $h(\Phi)$ is the Bernoulli "constant" along the field line $\Phi =$ constant. Poisson's equation now reads

$$\frac{1}{r^2} \frac{\partial}{\partial r} \left[r^2 \left(\frac{dh}{d\Phi} \frac{\partial \Phi}{\partial r} - K\rho^{-(2-\Gamma)} \frac{\partial \rho}{\partial r} \right) \right] + \frac{1}{r^2 \sin^2 \theta} \frac{\partial}{\partial \theta} \left[\sin \theta \left(\frac{dh}{d\Phi} \frac{\partial \Phi}{\partial \theta} - K\rho^{-(2-\Gamma)} \frac{\partial \rho}{\partial \theta} \right) \right] = 4\pi G\rho , \tag{4}$$

whereas force balance across field lines reads

$$\frac{1}{16\pi^3 r^2 \sin^2 \theta} \left(\frac{\partial^2 \Phi}{\partial r^2} + \frac{1}{r^2} \frac{\partial^2 \Phi}{\partial \theta^2} - \frac{\cot \theta}{r^2} \frac{\partial \Phi}{\partial \theta} \right) = -\rho \frac{dh}{d\Phi} . \tag{5}$$

We look for scale-free solutions of the above equations by nondimensionalizing and separating variables:

$$\rho = \left(\frac{K}{2\pi G r^2} \right)^{1/(2-\Gamma)} R(\theta) , \tag{6a}$$

$$\Phi = 4 \left(\frac{\pi^{3-2\Gamma} K r^{4-3\Gamma}}{G^{\Gamma/2}} \right)^{1/(2-\Gamma)} \phi(\theta) , \tag{6b}$$

$$\frac{dh}{d\Phi} = H_0 \left(\frac{2^{3\Gamma-2} K G^{2-2\Gamma}}{\pi^{1-\Gamma} \Phi^{2-\Gamma}} \right)^{1/(4-3\Gamma)} , \tag{6c}$$

where H_0 is a dimensionless constant that measures the deviation from a force-free magnetic field and $R(\theta)$ and $\phi(\theta)$ are dimensionless functions of the polar angle θ.[8] These assumptions imply that the equilibria will have spatially constant mass-to-flux ratios (see below). Substitution of equation (6c) into equations (4) and (5) yields

$$\frac{1}{\sin\theta}\frac{d}{d\theta}\{\sin\theta[A_\Gamma H_0\phi^{-(2-\Gamma)/(4-3\Gamma)}\phi' - R^{-(2-\Gamma)}R']\} = 2\left[R - \frac{(4-3\Gamma)}{(2-\Gamma)^2}R^{-(1-\Gamma)} - \left(\frac{4-3\Gamma}{2-\Gamma}\right)^2 B_\Gamma H_0\phi^{2(1-\Gamma)/(4-3\Gamma)}\right], \quad (7)$$

and

$$\frac{1}{\sin^2\theta}\left[\phi'' - \cot\theta\phi' + \frac{2(4-3\Gamma)(1-\Gamma)}{(2-\Gamma)^2}\phi\right] = -C_\Gamma H_0 R\phi^{-(2-\Gamma)/(4-3\Gamma)}, \quad (8)$$

where a prime denotes differentiation with respect to θ and

$$A_\Gamma = 2^{\Gamma(3-2\Gamma)/(4-3\Gamma)(2-\Gamma)}, \quad (9a)$$

$$B_\Gamma = 2^{-(1-\Gamma)(8-5\Gamma)/(4-3\Gamma)(2-\Gamma)}, \quad (9b)$$

$$C_\Gamma = 2^{-\Gamma(1-\Gamma)/(4-3\Gamma)(2-\Gamma)}. \quad (9c)$$

In particular, for $H_0 = 0$, equation (7) gives the dimensionless density for the nonmagnetized singular polytropic sphere

$$R = \left[\frac{4-3\Gamma}{(2-\Gamma)^2}\right]^{1/(2-\Gamma)}, \quad (10)$$

whereas equation (8) implies $\Phi = 0$ for $0 < \Gamma \leq 1$ in order to satisfy the boundary conditions given in equation (11). In this case, the mass-to-flux ratio λ_r is infinite. However, for $\Gamma = 0$, equation (8) admits also the analytic solution of $\Phi \propto r^2 \sin^2\theta$ corresponding to a straight and uniform field, while the density function is $R(\theta) = 1$. Therefore, a spherical logatropic scale-free cloud can be magnetized with a uniform magnetic field of any strength, and any value of the spherical mass to flux ratio is allowed.[9]

For arbitrary values of Γ and H_0, the ordinary differential equations (ODEs) (7) and (8) are to be integrated subject to the two-point boundary conditions (BCs):

$$\lim_{\theta\to 0}\sin\theta[A_\Gamma H_0\phi^{-(2-\Gamma)/(4-3\Gamma)}\phi' - R^{-(2-\Gamma)}R'] = 0,$$

$$\phi(0) = 0, \quad \phi'(\pi/2) = 0, \quad R'(\pi/2) = 0. \quad (11)$$

The first BC implies that there is no contribution from the polar axis to the mass inside a radius r. The second BC comes from the definition of magnetic flux, i.e., that there is no trapped flux at the polar axis. The last two BCs imply no kinks at the midplane.

The equilibria are characterized by the following:

1. The spherical mass-to-flux ratio,[10]

$$\lambda_r \equiv 2\pi G^{1/2}\frac{M(r)}{\Phi(r,\pi/2)} = 2^{(1-\Gamma)/(2-\Gamma)}\left(\frac{2-\Gamma}{4-3\Gamma}\right)\frac{1}{\phi(\pi/2)}\int_0^{\pi/2} R(\theta)\sin\theta\,d\theta, \quad (12)$$

where $M(r)$ is the mass enclosed within a radius r.

2. The factor D by which the average density is enhanced over the nonmagnetized value because of the extra support provided by magnetic fields,

$$D \equiv \left[\frac{4-3\Gamma}{(2-\Gamma)^2}\right]^{-1/(2-\Gamma)}\int_0^{\pi/2} R(\theta)\sin\theta\,d\theta, \quad (13)$$

which is equal to 1 if $H_0 = 0$ (see eq. [10]).

3. The sound speed

$$c_s^2 = (2\pi G r^2)^{(1-\Gamma)/(2-\Gamma)}K^{1/(2-\Gamma)}R(\theta)^{-(1-\Gamma)}. \quad (14)$$

4. The Alfvén speed,

$$v_A^2 = 2^{\Gamma/(2-\Gamma)}(2\pi G r^2)^{(1-\Gamma)/(2-\Gamma)}K^{1/(2-\Gamma)} \times \left[(\phi')^2 + \left(\frac{4-3\Gamma}{2-\Gamma}\right)^2\phi^2\right]\frac{1}{R(\theta)\sin^2\theta}. \quad (15)$$

Both the sound speed and the Alfvén speed scale as r^0 for $\Gamma = 1$ and as $r^{1/2}$ for $\Gamma = 0$; for other values of Γ, the exponent of r lies between these two values.

It is also of interest to define the ratio μ^2 of the square of the sound speed and the square of the Alfvén speed, each weighted by the density, which is a physical quantity that can be compared with observations:

$$\mu^2 = \frac{\int_0^{\pi/2} c_s^2\rho\sin\theta\,d\theta}{\int_0^{\pi/2} v_A^2\rho\sin\theta\,d\theta} = 2^{-\Gamma/(2-\Gamma)}\frac{\int_0^{\pi/2} R(\theta)^\Gamma\sin\theta\,d\theta}{\int_0^{\pi/2}\{(\phi')^2 + [(4-3\Gamma)/(2-\Gamma)]^2\phi^2\}/\sin\theta\,d\theta}. \quad (16)$$

If c_s represents only the thermal sound speed, then the observational summary given by Fuller & Myers (1992) would imply that $\mu^2 \sim 1$ in the quiet low-mass cores of giant molecular clouds (GMCs), whereas $\mu^2 \sim 10^{-2}$ in their envelopes. If we include in c_s, however, the turbulent contribution, then the turbulent speed is likely to be sub-Alfvénic or marginally Alfvénic, and $\mu^2 \lesssim 1$ everywhere is probably a better characterization of realistic clouds.

3. RESULTS

To obtain an equilibrium configuration for given values of Γ and H_0, equations (7) and (8) are integrated numerically. The integration is started at $\theta = 0$ using the expansions $\phi = a_0\xi^2 + \cdots$, $R = b_0 + b_2\xi^{4(1-\Gamma)/(4-3\Gamma)} + \cdots$, with $\xi = \sin\theta$ and $b_2 = [(4-3\Gamma)/2(1-\Gamma)]A_\Gamma H_0 a_0^{2(1-\Gamma)/(4-3\Gamma)}b_0^{2-\Gamma}$. The values of a_0 and b_0 are varied until the two BCs at $\theta = \pi/2$ (eq. [11]) are satisfied. For flattened equilibria (see below) it is more convenient to

[8] These definitions are not applicable for $\Gamma = 4/3$ or $\Gamma = 2$.

[9] In this case, $\lambda_r^2 = 2\mu^2 = [2\phi(\pi/2)^2]^{-1}$.

[10] The standard mass-to-flux ratio $\lambda = 2\pi G^{1/2}M(\Phi)/\Phi$ is not defined for the polytropic scale-free magnetized equilibria because the integral $\int_0^{\pi/2} R(\theta)\phi(\theta)^{-1}\sin\theta\,d\theta$ diverges since it can be shown that $R(\theta = 0) \neq 0$ for $\Gamma < 1$.

start from $\theta = \pi/2$, where the BCs $\phi'(\pi/2) = 0$ and $R'(\pi/2) = 0$ are imposed, and integrate toward $\theta = 0$. The values of $\phi(\pi/2)$ and $R(\pi/2)$ are then varied until a solution is found that satisfies the two BCs at $\theta = 0$.

Figure 1 shows the resulting flux and density functions $\phi(\theta)$ and $R(\theta)$ computed for $H_0 = 0.5$ and values of Γ between 0.2 and 1. We reproduce the results of Li & Shu (1996) for $\Gamma = 1$, which is the only case that obtains perfect toroids (i.e., $R[\theta = 0] = 0$); models with $\Gamma < 1$ have nonzero density at the polar axis. Figure 2 shows the corresponding density contours and magnetic field lines. In the limit $\Gamma \to 0$, independent of H_0 as long as it is nonzero, the pivotal configurations become thin disks with an ever increasing magnetic field strength. Table 1 shows the spherical mass to flux ratio λ_r, the overdensity parameter D, and the ratio of the square of the sound and Alfvén speeds μ^2. This table shows that, for fixed H_0, μ^2 decreases as Γ decreases because the magnetic field becomes stronger. For the same reason D increases. In contrast, λ_r goes through a minimum as Γ decreases. Figures 1 and 2 demonstrate that for $\Gamma \to 0$ (the logatropic limit), H_0 is not a measure of the strength of the magnetic fields since ϕ diverges as $R(\theta) \to \delta(\pi/2 - \theta)$ (see § 5 below).

For fixed Γ, a sequence from small H_0 to large H_0 progresses through configurations of increasing support by magnetic fields, as demonstrated explicitly for the isothermal case by Li & Shu (1996). This behavior is illustrated

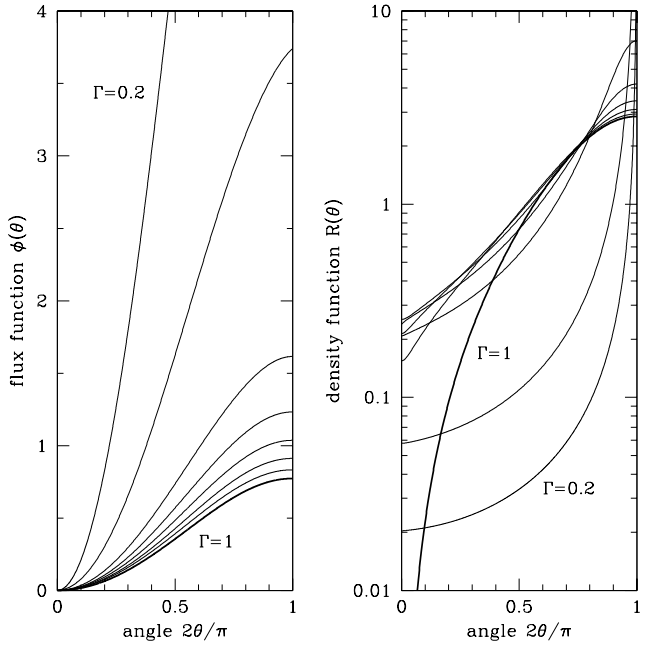

FIG. 1.—Flux and density functions $\phi(\theta)$ and $R(\theta)$ computed for $H_0 = 0.5$ and $\Gamma = 1$, 0.8, 0.7, 0.6, 0.5, 0.4, 0.3, and 0.2. The isothermal case is indicated by thick lines.

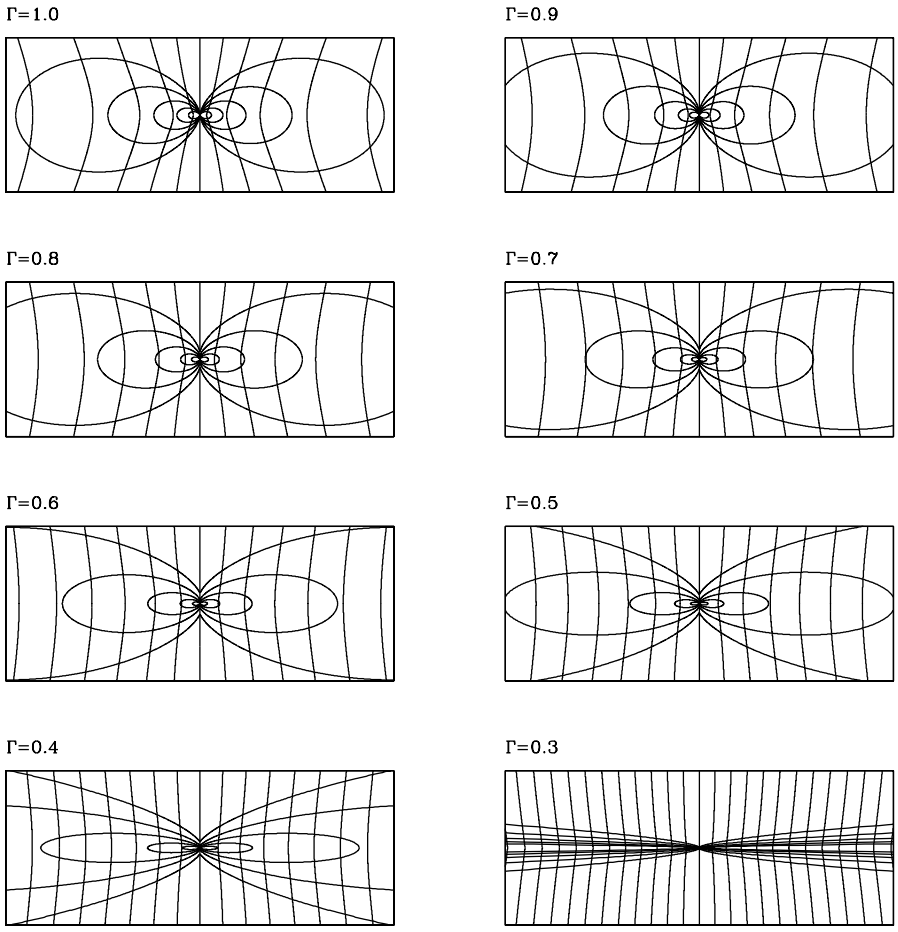

FIG. 2.—Density contours and magnetic field lines for $H_0 = 0.5$ and $\Gamma = 1$, 0.9, 0.8, 0.7, 0.6, 0.5, 0.4, 0.3, and 0.2. The isodensity levels correspond to $R(\theta) = 2^k$, and the isoflux contours correspond to $\phi(\theta) = (0.2k)^2$, where $k = 0, 1, 2, \ldots$.

TABLE 1

PARAMETERS OF EQUILIBRIA WITH $H_0 = 0.5$

Γ	λ_r	D	μ^2
1.....	1.94	1.50	0.668
0.9.....	1.80	1.68	0.632
0.8.....	1.63	1.76	0.543
0.7.....	1.45	1.80	0.434
0.6.....	1.27	1.84	0.321
0.5.....	1.09	1.91	0.218
0.4.....	0.927	2.14	0.122
0.3.....	0.947	5.06	0.0165
0.2.....	0.992	13.8	0.00181

here for the $\Gamma = 1/2$ case in Figure 3, which shows the density contours and magnetic field lines corresponding to values of H_0 from 0.05 to 1.5. Table 2 shows the corresponding values of λ_r, D, and μ^2. For small H_0, the equilibria have nearly spherically symmetric isodensity contours and weak quasi-uniform magnetic fields that provide little support against gravity. With increasing H_0, the pivotal configurations flatten. The case $H_0 = 1.5$ is already quite disklike: the pole-to-equator density contrast is $R(\pi/2)/R(0) \simeq 10^6$. For a thin disk, the analysis of Shu & Li (1997) demonstrates that magnetic tension provides virtually the sole means of horizontal support against self-gravity, with gas and magnetic pressures being important only for the vertical structure. In the limit of a completely flattened disk ($H_0 \to \infty$), $\lambda_r \to 1$ independent of the detailed nature of the gas EOS (see next section). Table 2 shows the spherical mass–to–flux ratio λ_r, the overdensity parameter D, and the ratio of the square of the sound and Alfvén speeds μ^2. Again D increases monotonically and μ^2 decreases monotonically

TABLE 2

PARAMETERS OF EQUILIBRIA WITH $\Gamma = 1/2$

H_0	λ_r	D	μ^2
0.....	∞	1	∞
0.05.....	4.35	1.18	6.93
0.1	2.83	1.21	2.81
0.2	1.85	1.31	1.08
0.3	1.45	1.45	0.577
0.4	1.23	1.64	0.348
0.5	1.09	1.91	0.218
0.6	1.01	2.34	0.134
0.7	0.980	3.00	0.0786
0.8	0.977	3.91	0.0448
0.9	0.982	4.95	0.0265
1.0	0.987	6.06	0.0165
1.1	0.991	7.22	0.0108
1.2	0.993	8.44	0.00733
1.3	0.995	9.71	0.00514
1.4	0.996	11.04	0.00369
1.5	0.997	12.42	0.00272

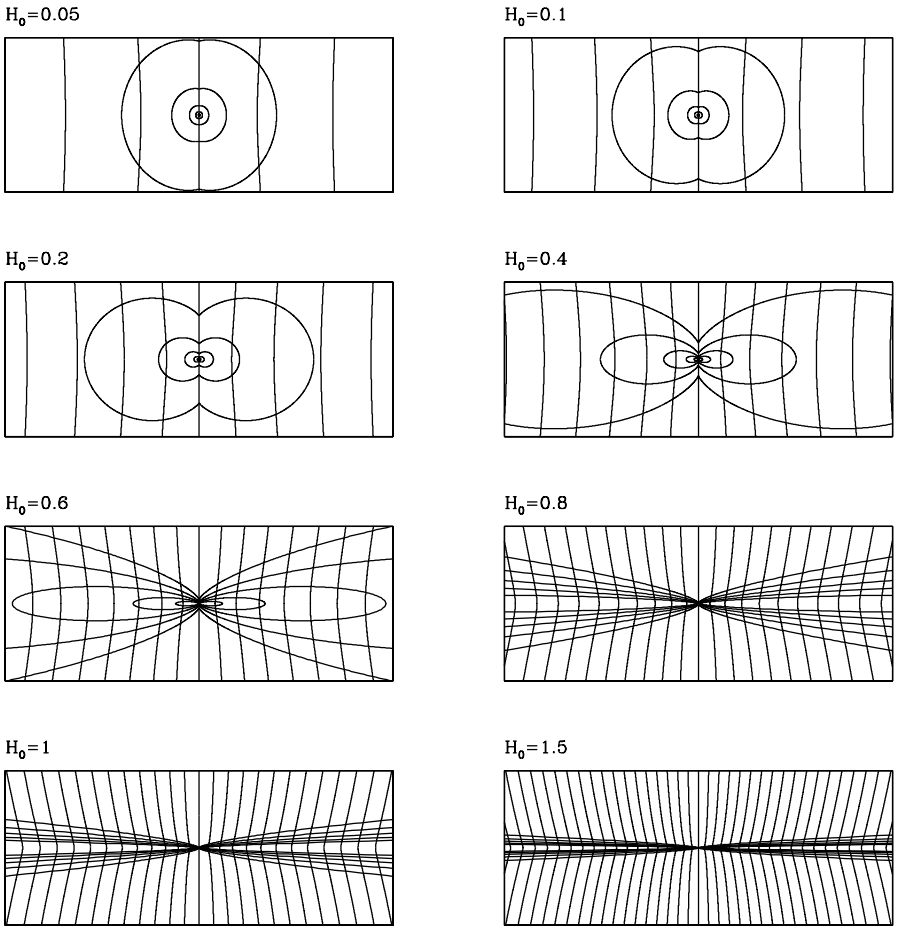

FIG. 3.—Density contours and magnetic field lines corresponding to $\Gamma = 1/2$ and $H_0 = 0.05$, 0.1, 0.2, 0.4, 0.6, 0.8, 1.0, and 1.5. The isodensity and isoflux contours are the same as in Fig. 2.

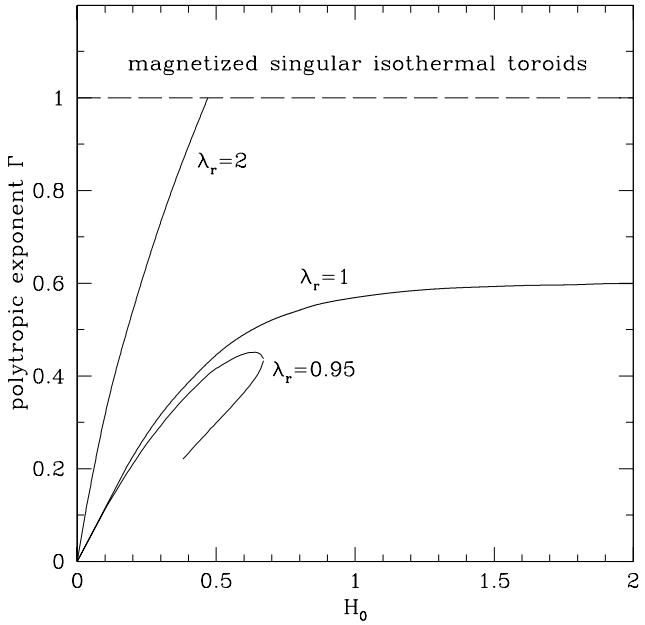

FIG. 4.—Locus of the set of equilibria with $\lambda_r = 0.95$, 1, and 2 in the (H_0, Γ)-plane.

as the magnetic support increases with H_0, while λ_r goes through a minimum and tends to 1 for large H_0.

Since the mass-to-flux ratio λ_r is a fundamental quantity that will not change unless magnetic field is lost by ambipolar diffusion, in Figure 4 we consider sequences where λ_r is held fixed but Γ is varied. This figure shows the locus of the set of equilibria with $\lambda_r = 0.95, 1,$ and 2 in the (H_0,Γ)-plane. Equilibria with $\lambda_r < 1$ are highly flattened when $\Gamma \to 0$, even for small but fixed values of H_0 (see § 6). In fact, to obtain incompletely flattened clouds when one takes the limit $\Gamma \to 0$, one also needs simultaneously to consider the limit $H_0 \to 0$. Unfortunately, because both the density and the strength of the magnetic field at the midplane diverge as the equilibria become highly flattened, we are unable to follow numerically the limit $\Gamma \to 0$ to verify whether these sequences of constant $\lambda_r < 1$ will hook to a finite value in the H_0-axis or will loop to $H_0 = 0$, consistent with our demonstration in § 4 that flattened disks do not exist in the logatropic limit.[11]

We speculate that the results for $\lambda_r < 1$ have the following physical interpretation. According to the theorem of Shu & Li (1997), only if λ itself rather than λ_r is less than unity is the magnetic field is strong enough overall to prevent the gravitational collapse of a highly flattened cloud. However, for moderate H_0 and Γ when $\lambda_r < 1$, even the singular equilibria are probably magnetically subcritical, since there can be little practical difference between the spherical mass-to-flux ratio λ_r and the "true" mass-to-flux ratio λ for highly flattened configurations. The latter is formally infinite when $\Gamma < 1$ only because the mass column goes to zero a little slower than the field column density when we perform an integration along the central field line (see footnote 10). In this interpretation, subcritical scale-free clouds with $\lambda_r < 1$ and intermediate values of Γ can become highly flattened because magnetic tension supports them laterally against their self-gravity while the soft EOS does not provide much resistance in the direction along the field lines. The squeezing of the cloud toward the mid-plane is compounded by the *confining* pressure of bent magnetic field lines that exert pinch forces in the vertical direction. Both the magnetic tension and the vertical pinch of magnetic pressure disappear when the field lines unbend, as they must to maintain the scale-free equilibria in the limit $\Gamma \to 0$ (see below). As a consequence, logatropic configurations become spherical for any value of λ_r. We leave as an interesting problem for future elucidation the determination of whether there is still a threshold in λ_r below which the SLS, embedded with straight and uniform field lines, will not collapse dynamically.

[11] As the equilibria flatten either as a result of small Γ or large H_0, it becomes necessary to determine the constants of the expansions of $R(\theta)$ and $\phi(\theta)$ near the origin with prohibitively increasing accuracy.

4. THE THIN-DISK LIMIT ($H_0 \gg 1$)

In the limit $H_0 \gg 1$, the cloud flattens to a thin disk for any $\Gamma \leq 1$. Dominant balance arguments applied to the two ODEs of the problem reveal the following asymptotic behavior:[12]

$$R(\theta) \to R_0\, \delta(\theta - \pi/2) H_0^{(4-3\Gamma)/(2-\Gamma)} + s(\theta) H_0^{-(4-3\Gamma)/(2-\Gamma)(1-\Gamma)}, \tag{17}$$

$$\phi \to f(\theta) H_0^{(4-3\Gamma)/(2-\Gamma)}. \tag{18}$$

To the lowest order in H_0 the equation of force balance along field lines (eq. [7]) becomes

$$\frac{1}{\sin\theta}\frac{d}{d\theta}\left[\sin\theta (A_\Gamma f^{-(2-\Gamma)/(4-3\Gamma)} f' - s^{-(2-\Gamma)} s')\right] = -2\left[\frac{4-3\Gamma}{(2-\Gamma)^2} s^{-(1-\Gamma)} + \left(\frac{4-3\Gamma}{2-\Gamma}\right) B_\Gamma f^{2(1-\Gamma)/(4-3\Gamma)}\right], \tag{19}$$

which is valid over the interval $0 \leq \theta < \pi/2$, plus the integral constraint

$$R_0 - \frac{4-3\Gamma}{(2-\Gamma)^2}\int_0^\pi s^{-(1-\Gamma)} \sin\theta\, d\theta - \left(\frac{4-3\Gamma}{2-\Gamma}\right)^2 B_\Gamma \int_0^\pi f^{2(1-\Gamma)/(4-3\Gamma)} \sin\theta\, d\theta = 0, \tag{20}$$

obtained by integrating equation (7) from $\theta = 0$ to π and applying the first boundary condition (eq. [11]) on the polar axis.

The constant R_0 is proportional to the surface density of the polytropic disks, given by

$$\Sigma(r) \equiv \lim_{\epsilon \to 0} \int_{\pi/2-\epsilon}^{\pi/2+\epsilon} \rho r \sin\theta\, d\theta \to \left(\frac{K}{2\pi G}\right)^{1/(2-\Gamma)} r^{-\Gamma/(2-\Gamma)} R_0 H_0^{(4-3\Gamma)/(2-\Gamma)}, \tag{21}$$

which, for $\Gamma = 1$, gives $\Sigma \to H_0 a^2/\pi G r$, as found by Li & Shu (1996).

Equation (8), which expresses force balance across field lines, reduces to

[12] These expansions are not valid for $\Gamma = 1$. See Li & Shu (1996) for the correct asymptotic expansion in this case.

$$\frac{1}{\sin^2\theta}\left[f'' - \cot\theta f' + l(l+1)f\right] = -C_\Gamma f^{-(2-\Gamma)/(4-3\Gamma)} R_0\,\delta(\theta - \pi/2)\,, \quad (22)$$

where the parameter l is defined by

$$l(l+1) \equiv \frac{2(4-3\Gamma)(1-\Gamma)}{(2-\Gamma)^2}\,. \quad (23)$$

This is equivalent to the equation for force-free magnetic fields,

$$f'' - \cot\theta f' + l(l+1)f = 0\,, \quad (24)$$

which is valid over the interval $0 \le \theta < \pi/2$, plus the condition

$$2f'(\pi/2) = C_\Gamma R_0 f(\pi/2)^{-(2-\Gamma)/(4-3\Gamma)}\,, \quad (25)$$

obtained by integrating equation (8) from $\pi/2 - \epsilon$ to $\pi/2 + \epsilon$ and taking the limit $\epsilon \to 0$. For integer l, solutions of equation (24), which is regular at $\theta = 0$, are Gegenbauer polynomials of order l and index $\frac{1}{2}$, $C_l^{1/2}$ (see e.g., Abramowitz & Stegun 1965). In general, it can be shown (Chandrasekhar 1955) that any axisymmetric force-free field, separable in spherical coordinates, can be expressed in terms of fundamental solutions whose radial dependence is given by a combination of Bessel functions of fractional order, and the angular dependence by Gegenbauer polynomials of index $\frac{1}{2}$. In our case, the choice of Γ determines a particular exponent of the power law for the radial part of the flux function, and hence the corresponding value of l (noninteger, except for $\Gamma = 0$ and 1).

Therefore, the magnetic field is force-free everywhere except at the midplane, where $\rho \neq 0$ and the condition of force balance across field lines has to be satisfied. In the thin-disk limit discussed here, the boundary condition $\phi'(\pi/2) = 0$ is clearly not fulfilled: the kink of ϕ at the midplane provides the magnetic support against self-gravity on the midplane. Currents must exist in the disk to support these kinks.

With the definitions

$$y(\theta) \equiv -A_\Gamma \frac{4-3\Gamma}{2} f(\theta)^{2(1-\Gamma)/(4-3\Gamma)}\,,$$

$$z(\theta) \equiv s(\theta)^{-(1-\Gamma)}\,,$$

equation (19) transforms into

$$z'' + \cot\theta z' + l(l+1)z = y'' + \cot\theta y' + l(l+1)y\,, \quad (26)$$

which has the solution

$$z(\theta) = y(\theta) + q(\theta)\,,$$

where $q(\theta)$ is a solution of the homogeneous equation

$$q'' + \cot\theta q' + l(l+1)q = 0\,. \quad (27)$$

Therefore,

$$s(\theta) = \left[q - A_\Gamma \frac{4-3\Gamma}{2} f^{2(1-\Gamma)/(4-3\Gamma)}\right]^{-1/(1-\Gamma)}\,, \quad (28)$$

and the integral constraint (eq. [20]), becomes

$$\int_0^{\pi/2} q(\theta)\sin\theta\,d\theta = \frac{(2-\Gamma)^2}{2(4-3\Gamma)} R_0\,. \quad (29)$$

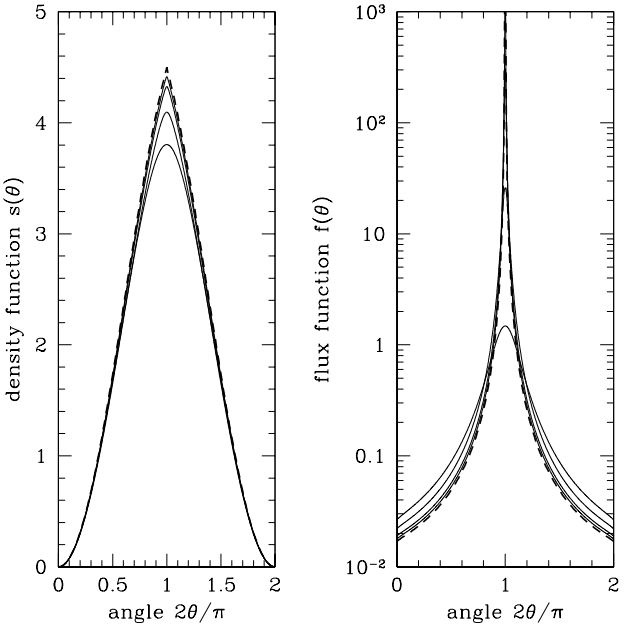

FIG. 5.—Functions $f(\theta)$ and $s(\theta)$ for $\Gamma = 1/2$ and $H_0 =$ 0.4, 0.6, 0.8, 1.0, 1.2, and 1.5, compared with the asymptotic expressions obtained for $H_0 \gg 1$, shown by the thick dashed lines. For clarity, the functions are shown over the range $0 \le \theta \le \pi$.

The problem is thus reduced to the solution of the two homogeneous equations (24) and (27) for the functions $f(\theta)$ and $q(\theta)$, which are determined up to an arbitrary constant. However, the two integral constraints that would have determined these latter constants (eqs. [25] and [29]) contain the additional unknown parameter R_0. The system of equations is closed by the requirement that

$$\lim_{H_0 \to \infty} \lambda_r = 1\,.$$

Substituting equations (17) and (18) in equation (12), one obtains

$$\lim_{H_0 \to \infty} \lambda_r = 2^{(1-\Gamma)/(2-\Gamma)}\left(\frac{2-\Gamma}{4-3\Gamma}\right)\frac{R_0}{2f(\pi/2)} = 1\,,$$

i.e.,

$$R_0 = 2^{1/(2-\Gamma)}\left(\frac{4-3\Gamma}{2-\Gamma}\right) f(\pi/2)\,, \quad (30)$$

which gives the remaining condition.

Equations (24) and (27) can be solved numerically by starting the integration at $\theta = 0$ with the series expansions: $q(\theta) = q_0[1 - \frac{1}{4}l(l+1)\theta^2 + \cdots]$ and $f(\theta) = f_0\{\theta^2 - \frac{1}{8}[l(l+1) + \frac{2}{3}]\theta^4 + \cdots\}$, where q_0 and f_0 are arbitrary constants.[13] The constants q_0, f_0, and R_0 are then determined by the constraints expressed by equations (20), (25), and (30).

Figure 5 shows the functions $f(\theta)$ and $s(\theta)$ obtained for $\Gamma = 1/2$ and increasing values of H_0 from 0.4 to 1.5 compared with the asymptotic expressions computed here. Already for $H_0 = 1.5$, the actual $f(\theta)$ and $s(\theta)$ are very close

[13] The two original BCs on the function $R(\theta)$ are of little use here: the one at $\theta = 0$ reduces to the condition $\lim_{\theta \to 0}(1-\Gamma)^{-1}\sin\theta q' = 0$, which is trivially satisfied; the second BC, $R'(\pi/2) = 0$, cannot be applied because of the δ-function at $\pi/2$.

TABLE 3

PARAMETERS FOR THE THIN-DISK LIMIT

Γ	α (deg)	$f(\pi/2)$	R_0
1.....	45	1	2
0.9.....	52	1.19	2.65
0.8.....	58	1.52	3.61
0.7.....	64	2.05	5.10
0.6.....	69	2.93	7.55
0.5.....	73	4.50	11.9
0.4.....	77	7.59	20.5
0.3.....	81	14.7	40.4
0.2.....	84	36.8	102
0.1.....	87	166	467
0.....	90	∞	∞

to the corresponding asymptotic functions given by equations (17) and (18). Table 3 shows the value of the angle α of the magnetic field with the plane of the disk, the flux function f evaluated at $\theta = \pi/2$ (indicative of the magnetic field strength), and the surface density parameter R_0 as functions of Γ. The angle α ranges from 45° for the isothermal case $\Gamma = 1$ to 90° in the logatropic case, $\Gamma = 0$. Correspondingly, the magnetic flux in the disk and the surface density both diverge as $\Gamma \to 0$ for any large but finite value of H_0.

5. THE QUASI-SPHERICAL LIMIT ($H_0 \ll 1$)

For the isothermal case $\Gamma = 1$, Li & Shu (1996) have shown how the SIS is recovered for $H_0 \ll 1$ from a family of toroids with zero density on the polar axis. For $\Gamma \neq 1$, in the limit $H_0 \ll 1$, the asymptotic expansions are given by

$$R(\theta) \to \left[\frac{4-3\Gamma}{(2-\Gamma)^2}\right]^{1/(2-\Gamma)} + p(\theta) H_0^{(4-3\Gamma)/(3-2\Gamma)} + \cdots,$$

$$\phi = g(\theta) H_0^{(4-3\Gamma)/2(3-2\Gamma)} + \cdots.$$

To the lowest order in H_0, equations (7) and (8) become

$$\frac{1}{\sin\theta}\frac{d}{d\theta}\left\{\sin\theta\left[A_\Gamma g^{-(2-\Gamma)/(4-3\Gamma)} g' - \frac{(2-\Gamma)^2}{4-3\Gamma} p'\right]\right\}$$

$$= 2\left[(2-\Gamma)p - \left(\frac{4-3\Gamma}{2-\Gamma}\right)^2 B_\Gamma g^{2(1-\Gamma)/(4-3\Gamma)}\right], \quad (31)$$

and

$$\frac{1}{\sin^2\theta}\left[g'' - \cot\theta g' + l(l+1)g\right]$$

$$= -C_\Gamma\left[\frac{4-3\Gamma}{(2-\Gamma)^2}\right]^{1/(2-\Gamma)} g^{-(2-\Gamma)/(4-3\Gamma)}. \quad (32)$$

The BCs for the functions $p(\theta)$ and $g(\theta)$ are the same as those for $R(\theta)$ and $\phi(\theta)$ in equation (11).

Figure 6 shows the convergence of the solutions of the full set of equations (7) and (8) obtained for $\Gamma = 1/2$ and decreasing values of H_0 from 0.4 to 0.05 to the asymptotic solutions obtained by integrating the equations above. Notice that $p(0) < 0$ and $p(\pi/2) > 0$ showing that the sequence of equilibria with $\Gamma = 1/2$ originates from the corresponding unmagnetized spherical state (eq. [10]) by reducing the density on the pole and enhancing it on the equator. The same behavior is found for any value of Γ in the range $0 < \Gamma < 1$. For $\Gamma = 1$, the function $p(\theta)$ diverges at $\theta = 0$, indicating that this expansion is not appropriate in the isothermal case, as in the case $H_0 \gg 1$. For the same reason, the expansion also fails for $\Gamma = 0$, since both $g(\theta)$ and $p(\theta)$ diverge on the equatorial plane.

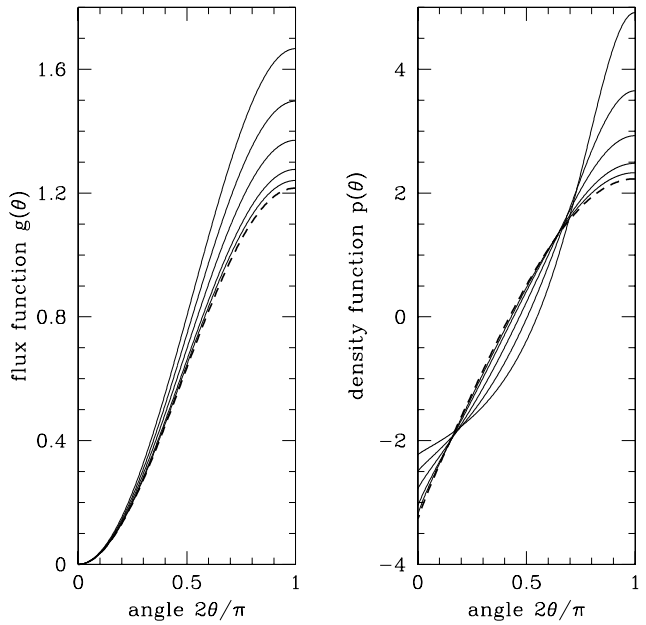

FIG. 6.—Functions $g(\theta)$ and $p(\theta)$ for $\Gamma = 1/2$ and $H_0 =$ 0.4, 0.3, 0.2, 0.1, and 0.05, compared with the asymptotic expressions obtained for $H_0 \ll 1$, shown by the thick dashed lines.

These flattened configurations are supported by magnetic and gas pressure against self-gravity. The intensity of the magnetic field can become very high even though H_0 is small because the latter parameter measures not the field strength but the deviations from a force-free field (see eq. [6c]).

6. THE LOGATROPIC LIMIT ($\Gamma \to 0$)

We consider in this section the logatropic limit $\Gamma \to 0$. As anticipated in § 2, for $\Gamma = 0$ equations (7) and (8) admit the analytical solution $R = 1$ and $\Phi \propto r^2 \sin^2\theta$, corresponding to a SLS threaded by a straight and uniform magnetic field. This solution represents the only possible scale-free isopedic configuration of equilibrium for a magnetized cloud with a logatropic EOS. To show this, we use the results of §§ 4 and 5 for $H_0 \gg 1$ and $H_0 \ll 1$ to find the limit of the equilibrium configurations for $\Gamma \to 0$ and fixed (small or large) values of H_0.

In the limit $H_0 \gg 1$, $\Gamma \to 0$, analytic solutions to equations (24) and (27) exist. The magnetic field tends to become uniform and straight, $f(\theta) \to f(\pi/2) \sin^2\theta$, but $f(\pi/2)$ diverges, as shown in Table 3, and therefore $s(\theta = \pi/2)$ also diverges (see eq. [28]). Equation (21) shows in this limit that the surface density Σ is independent of r, and therefore no pressure gradients can be exerted in the horizontal direction. The value $\Sigma = (K/2\pi G)^{1/2} R_0 H_0^2$ diverges as $\Gamma \to 0$ for any value of H_0 because $\lim_{\Gamma \to 0} R_0 = \infty$ (see Table 3). The magnetic flux threading the disk, $\phi = 2^{-3/2} R_0 H_0^2 r^2 \sin^2\theta$, becomes infinite in order to keep the mass to flux ratio λ_r equal to 1. Therefore, the limiting configuration approaches a uniform disk with infinite surface density, threaded by an infinitely strong uniform and straight magnetic field.

If we now examine the case $H_0 \ll 1$, in the limit $\Gamma \to 0$, it is easy to show from equation (32) that the magnetic field tends to become uniform, $g(\theta) \to g(\pi/2) \sin^2 \theta$, but $\lim_{\Gamma \to 0} g(\pi/2) = \infty$. Consequently, the density function $p(\theta)$ also diverges in $\theta = \pi/2$, and the configuration again approaches a thin disk threaded by an uniform, infinitely strong, magnetic field.

We conclude that scale-free logatropic clouds cannot exist as magnetostatic disks except in some limiting configuration. In the absence of such limits, the equilibria are spherical and can be magnetized only by straight and uniform field lines; i.e., the magnetic field is force free and therefore is given by $H_0 = 0$. The inside-out gravitational collapse of such a SLS would still proceed self-similarly as in the solution of McLaughlin & Pudritz (1997), but the frozen-in magnetic fields would yield a dependence with polar angle that eventually produces a pseudodisk (Galli & Shu 1993a, 1993b; Allen & Shu 1998a).

7. SUMMARY AND DISCUSSION

We have solved the scale-free equations of magnetostatic equilibrium of isopedic self-gravitating polytropic clouds to find pivotal states that represent the initial state for the onset of dynamical collapse, as first proposed by Li & Shu (1996) for isothermal clouds. Compared to unmagnetized equilibria, the magnetized configurations are flattened because of magnetic support across field lines. The degree of this support is best represented by the ratio of the square of the sound to Alfvén speeds μ^2, or the overdensity parameter D, since they are always monotonic functions of H_0 and Γ.

Configurations with $\Gamma = 1$ become highly flattened as the parameter H_0 increases. When $\Gamma < 1$ (softer EOS) the equilibria get flattened even faster at the same values of H_0, since along field lines there is less support from a soft EOS than for a stiff one. However, it seems that in the logatropic limit flattened disks do not exist: the singular scale-free equilibria can only be spherical uniformly magnetized clouds. Figure 7 shows a schematic picture of the (H_0, Γ)-plane indicating the topology of the solutions for scale-free magnetized isopedic singular self-gravitating clouds.

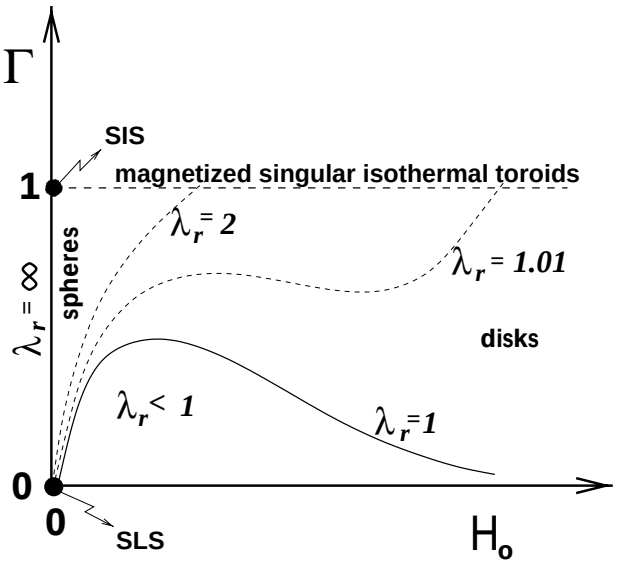

FIG. 7.—Schematic picture of the (H_0, Γ)-plane indicating the topology of the solutions for scale-free magnetized isopedic singular self-gravitating clouds.

In self-gravitating clouds, the joint compression of matter and field is often expressed as producing an expected relationship: $B \propto \rho^\kappa$, with different theorists expressing different preferences for the value of κ (e.g., Mestel 1965; Fiedler & Mouschovias 1993). No local (i.e., point by point) relationship of the form $B \propto \rho^\kappa$ holds for the scale-free equilibria studied in this paper. However, if we average the magnetic field strength and mass density over ever larger spherical volumes centered on $r = 0$, we do recover such a relationship: $\langle B \rangle \propto \langle \rho \rangle^\kappa$, where angle brackets denote the result of such a spatial average and $\kappa = \Gamma/2$.

We may think of the result $\langle B \rangle \propto \langle \rho \rangle^{\Gamma/2}$ as arising physically from a combination of two tendencies: (1) Slow cloud contraction in the absence of magnetic fields and rotation tends to keep roughly one Jeans mass inside every radius r, which yields $\langle \rho \rangle \propto \langle c_s^2 \rangle / G r^2$, or $\langle \rho \rangle \propto r^{-2/(2-\Gamma)}$ if $\langle c_s^2 \rangle \propto \langle \rho \rangle^{\Gamma - 1}$. (2) Slow cloud contraction in the absence of gas pressure tends to keep roughly one magnetic critical mass inside every radius r, which yields $\langle B \rangle / r \langle \rho \rangle \propto \lambda_r =$ constant, or $\langle B \rangle \propto r \langle \rho \rangle \propto r^{-\Gamma/(2-\Gamma)} \propto \langle \rho \rangle^{\Gamma/2}$ if gas pressure (thermal or turbulent) plays a comparable role to magnetic fields in cloud support. Notice that our reasoning does not rely on arguments of cloud geometry, e.g., whether cloud cores flatten dramatically or not as they contract; nor does it depend sensitively on the precise reason for core contraction, e.g., because of ambipolar diffusion or turbulent decay.

Crutcher (1998) claims that the observational data are consistent with $\kappa = 0.47 \pm 0.05$. If we take Crutcher's conclusion at face value, we would interpret the observations as referring mostly to regions where the EOS is close to being isothermal $\Gamma \approx 1$, which is the approximation adopted by many theoretical studies that ignore the role of cloud turbulence. The result is not unexpected for low-mass cloud cores, but we would not naively have expected this relationship for high-mass cores and cloud envelopes, where the importance of turbulent motions is much greater. Unfortunately, the observational data refer to different clouds rather than to different (spatially averaged) regions of the same cloud, so there is some ambiguity how to make the proper connection to different theoretical predictions. There may also be other mechanisms at work, e.g., perhaps a tendency for observations to select for regions of nearly constant Alfvén speed, $\langle v_A \rangle \propto \langle B \rangle / \langle \rho \rangle^{1/2} \approx$ constant (Bertoldi & McKee 1992). Thus, we would warn the reader against drawing premature conclusions about the effective EOS for molecular clouds, or the related degree to which observations can at present distinguish whether molecular clouds are magnetically supercritical or subcritical.

If molecular clouds are magnetically supercritical, with λ_r greater than 1 by order unity (say, $\lambda_r = 2$), then an appreciable fraction (say, 1/2) of their support against self-gravity has to come from turbulent or thermal pressure (Elmegreen 1978; McKee et al. 1993; Crutcher 1998). Modeled as scale-free equilibria, such clouds with μ^2 of order unity are not highly flattened (see Tables 1 and 2 and Figs. 2 and 3). Suppose we try gravitationally to extract a subunit from an unflattened massive molecular cloud, where the cloud as a whole is only somewhat supercritical, $\lambda_r \sim 2$. If the subunit's linear size is smaller than the vertical dimension of the cloud by more than a factor of 2, which will be the case if we consider subunits of stellar mass scales, then this subunit will not itself be magnetically supercritical. Magnetically subcritical pieces of clouds cannot contract indefinitely

without flux loss, so star formation in *unflattened* clouds, if they are not highly supercritical, needs to invoke some degree of ambipolar diffusion in order to produce small dense cores that can gravitationally separate from their surroundings.

On the other hand, if molecular clouds are magnetically critical or subcritical, with $\lambda_r \leq 1$, then almost all scale-free equilibria are highly flattened, with μ^2 appreciably less than unity. On a small scale, any subunit of this cloud, even subunits with vertical dimension comparable to the cloud as a whole, would also be magnetically critical or subcritical. For such a subunit to contract indefinitely, we would again need to invoke ambipolar diffusion to make a cloud core magnetically supercritical. Thus, although the decay of turbulence can accelerate the formation of cloud cores, the ultimate formation of stars from such cores may still need to rely on *some* magnetic flux loss (but perhaps not more than a factor of ~ 2) to trigger the evolution of the cores toward gravomagneto catastrophe and a pivotal state with a formally infinite central concentration.

On the large scale, Shu & Li (1997) proved that if GMCs are modeled as flattened isopedic sheets, magnetic pressure and tension are proportional to the gas pressure and force of self-gravity. Their theorems hold independently of the detailed forms of the EOS or the surface density distribution. If GMCs are truly highly flattened—with typical dimensions, say, of 50 pc × 50 pc × a few pc, or even less—then many aspects of their magnetohydrodynamic stability and evolution become amenable to a simplified analysis through the judicious application and extension of the theorems proved by Shu & Li (1997) (see, e.g., Allen & Shu 1998b; Shu et al. 1999). This exciting possibility deserves further exploration.

D. G. acknowledges support by CNR grant 97.00018.CT02, ASI grant ARS-96-66 and ARS-98-116, and hospitality from UNAM, México. S. L. acknowledges support by J. S. Guggenheim Memorial Foundation, grants DGAPA-UNAM and CONACyT, and hospitality from Osservatorio di Arcetri. F. C. A. is supported by NASA grant NAG 5-2869 and by funds from the physics department at the University of Michigan. The work of F. H. S. is supported in part by an NSF grant and in part by a NASA theory grant awarded to the Center for Star Formation Studies, a consortium of the University of California at Berkeley, the University of California at Santa Cruz, and the NASA Ames Research Center.

REFERENCES

Abramowitz, M., & Stegun, I. A. 1965, Handbook of Mathematical Functions (New York: Dover)
Allen, A., & Shu, F. H. 1998a, in preparation
———. 1998b, in preparation
Barker, D. M., & Mestel, L. 1996, MNRAS, 282, 317
Barranco, J. A., & Goodman, A. A. 1998, ApJ, 504, 207
Basu, S., & Mouschovias, T. C. 1994, ApJ, 432, 720
Bertoldi, F., & McKee, C. F. 1992, ApJ, 395, 140
Caselli, P., & Myers, P. C. 1995, ApJ, 446, 665
Chandrasekhar, S. 1955, Proc. Nat. Acad. Sci., 42, 1
Cheng, A. F. 1978, ApJ, 221, 320
Ciolek, G. E., & Königl, A. 1998, ApJ, 504, 257
Ciolek, G. E., & Mouschovias, T. Ch. 1994, ApJ, 425, 142
Crutcher, R. M. 1998, ApJ, submitted
Dame, T., Elmegreen, B. G., Cohen, R., & Thaddeus, P. 1986, ApJ, 305, 892
Elmegreen, B. G. 1978, ApJ, 225, L85
Falgarone, E., Puget, J.-L., & Pérault, M. 1992, AA, 257, 715
Fatuzzo, M., & Adams, F. C. 1993, ApJ, 412, 146
Fiedler, R. A., & Mouschovias, T. Ch. 1993, ApJ, 415, 680
Field, G. B., Goldsmith, D. W., & Habing, H. J. 1969, ApJ, 158, 173
Fuller, G. A., & Myers, P. C. 1992, ApJ, 384, 253
Galli, D., & Shu, F. H. 1993a, ApJ, 417, 220
———. 1993b, ApJ, 417, 243
Gammie, C. F., & Ostriker, E. C. 1996, ApJ, 466, 814
Holliman, J. H., & McKee, C. F. 1993, BAAS, 182, 61.11
Larson, R. B. 1981, MNRAS, 194, 809
Leung, C., Kutner, M., & Mead, K. 1982, ApJ, 262, 583
Li, Z.-Y., & Shu, F. 1996, ApJ, 472, 211
———. 1997, ApJ, 475, 237
Lizano, S., & Shu, F. H. 1989, ApJ, 342, 834
Mac Low, M. M., Klessen, R. S., Burkert, A., Smith, M. D., & Kessel, O. 1998, Phys. Rev. Lett. 80, 2754
Maloney, P. 1988, ApJ, 334, 761
McKee, C. F., & Zweibel, E. G. 1995, ApJ, 440, 686
McKee, C. F., Zweibel, E. G., Goodman, A. A., & Heiles, C. 1993, in Protostars and Planets III, ed. E. H. Levy & J. I. Lunine (Tucson: Univ. Arizona Press), 327
McLaughlin, D. E., & Pudritz, R. E. 1996, ApJ, 469, 194
———. 1997, ApJ, 476, 750
Mestel, L. 1965, QJRAS, 6, 265
Mestel, L., & Spitzer, L. 1956, MNRAS, 116, 505
Mestel, L., & Strittmatter, P. A. 1967, MNRAS, 137, 95
Miesch, M. S., & Bally, J. 1994, ApJ, 429, 645
Myers, P. C., & Benson, P. J. 1983, ApJ, 266, 309
Myers, P. C., & Fuller, G. A. 1992, ApJ, 396, 631
Myers, P. C., & Lazarian, A. 1998, ApJ, 507, L157
Nakano, T. 1979, PASJ, 31, 697
Nakano, Y. 1998, ApJ, 494, 587
Ostriker, E. C., Gammie, C. F., & Stone, J. M. 1999, ApJ, 513, 259
Padoan, P., & Nordlund, A. 1999, ApJ, submitted
Pikel'ner, S. B. 1967, AZh., 44, 1915
Shu, F. H., Adams, F. C., & Lizano, S. 1987, ARA&A, 25, 23
Shu, F. H., Allen, A., Shang, H., Ostriker, E. C., & Li, Z. Y. 1999, in The Physics of Star Formation and Early Stellar Evolution II, ed. C. J. Lada & N. D. Kylafis (Dordrecht: Kluwer), in press
Shu, F. H., & Li, Z.-Y. 1997, ApJ, 475, 251
Shu, F. H., Milione, V., Gebel, W., Yuan, C., Goldsmith, D. W., & Roberts, W. W. 1972, ApJ, 173, 557
Spitzer, L., & Scott, E. H. 1969, ApJ, 158, 185
Stone, J. M, Ostriker, E. C., & Gammie, C. F. 1998, ApJ, 508, L99
Tomisaka, K., Ikeuchi, S., & Nakamura, T. 1989, ApJ, 341, 220
Torrelles, J. M., Rodríguez, L. F., Cantó, J., Carral, P., Marcaide, J., Morán, J. M., & Ho, P. T. P. 1983, ApJ, 274, 214
Vázquez-Semadeni, E., Cantó, J., & Lizano, S. 1998, ApJ, 492, 596
Viala, Y. P., & Horedt, G. P. 1974, A & A, 33, 195
Vishniac, E. T., & Lazarian, A. 1999, ApJ, 511, 193
Walén, C. 1944, Ark. Mat. Astron. Fys. 30A, 15, 1
Weinberg, S. 1962, Phys. Rev., 126, 1899